Joint Diseases and Related Surgery

Jt Dis Relat Surg
2026;37(2):489-500

ORIGINAL ARTICLE

Optimizing fixation in medial distal femur fractures: A biomechanical study

Atahan Durgal, MD[1], Enver Kilic, MD[1], Elif Naz Perdeci, MSc[2], Fatma Kubra Erbay Elibol[2], Taner Karlidag, MD[3], Burak Kulakoglu, MD[4], Teyfik Demir[5], Olgun Bingol, MD[1], Guzelali Ozdemir, MD[1]

[1]Department of Orthopedics and Traumatology, Ankara Bilkent City Hospital, Ankara, Türkiye
[2]Department of Biomedical Engineering, TOBB University of Economics and Technology, Ankara, Türkiye
[3]Department of Orthopedics and Traumatology, Gaziantep City Hospital, Gaziantep, Türkiye
[4]Department of Orthopedics and Traumatology, Antalya City Hospital, Antalya, Türkiye
[5]Department of Mechanical Engineering, TOBB University of Economics and Technology, Ankara, Türkiye

Distal femur fractures, although relatively uncommon, pose significant clinical challenges, particularly when they involve unicondylar patterns. Unicondylar variants are particularly rare, comprising only ~0.65% of cases.[1-3] Medial femoral condyle fractures (AO/OTA 33-B2.1), in contrast to their more frequently encountered lateral counterparts, are exceedingly rare and often underrepresented in literature.[4] These injuries frequently result from high-energy trauma or low-energy mechanisms in osteoporotic bone, necessitating precise anatomic reduction and stable internal fixation to restore joint congruity and enable early mobilization.[1,5] Despite advancements in fixation strategies, no consensus exists regarding

Received: August 09, 2025
Accepted: November 19, 2025
Published online: March 20, 2026

Correspondence: Atahan Durgal, MD. Ankara Bilkent Şehir Hastanesi, Ortopedi ve Travmatoloji Kliniği, 06800 Çankaya, Ankara, Türkiye.

E-mail: durgalatahan016@gmail.com

Doi: 10.52312/jdrs.2026.2543

Citation: Durgal A, Kilic E, Perdeci EN, Erbay Elibol FK, Karlidag T, Kulakoglu B, et al. Optimizing fixation in medial distal femur fractures: A biomechanical study. Jt Dis Relat Surg 2026;37(2):489-500. doi: 10.52312/jdrs.2026.2543.

ABSTRACT

Objectives: This study aims to biomechanically compare four fixation methods to identify the most stable construct under axial loading conditions.

Material and methods: A standardized osteotomy model simulating AO/OTA 33-B2.1 fractures was created in 28 synthetic femurs. Four groups (n = 7 each) were tested: (1) three 6.5-mm cannulated screws, (2) the same with an additional centrally placed screw, (3) three screws plus a 3.5-mm buttress plate, and (4) three screws combined with a reversed anatomical proximal tibial locking plate. Constructs were subjected to cyclic and static axial loading. The prespecified primary endpoint was load at 2-mm displacement, with stiffness and maximum load to failure as secondary outcomes.

Results: Group 4 exhibited the highest stiffness (802 ± 70 N/mm), maximum load (2360 ± 389 N), and resistance to 2-mm displacement (1138 ± 87 N). Group 2, with a centrally placed fourth screw, showed significantly improved performance in terms of maximum load compared to the traditional three-screw construct. While Group 3 improved stiffness over screw-only constructs, it did not significantly outperform Group 2 in key load metrics. Group 2, with a centrally placed fourth screw, demonstrated comparable stability to the buttress plate and anatomical locking plate in selected metrics, but remained inferior to the locking plate construct.

Conclusion: Central placement of cannulated screws to the medial femoral condyle enhanced axial stability in this synthetic model and represented a minimally invasive alternative to buttress plating in selected metrics. The highest stability was achieved with the combined use of cannulated screws and a locking plate. These results are restricted to axial loading and the tested endpoints; thus, further biomechanical, cadaveric, and clinical studies are warranted before generalizing to early weight-bearing. Given the anatomical challenges of the medial condyle, the development of anatomically contoured locking plates specifically designed for this region remains an important future direction.

Keywords: AO 33-B2.1, mechanical study, medial femoral condyle fracture, synthetic bone, unicondylar distal femur fractures.

the optimal implant configuration for medial condylar involvement.[6-8]

Achieving precise anatomic reduction and stable internal fixation remains an absolute requirement in the management of all intra-articular fractures. With increasing life expectancy and rising functional demands among patients, the concept of stability has become more critical than ever-particularly in light of treatment failures encountered in various clinical scenarios. Standard treatment methods have included interfragmentary lag screw fixation, often supplemented by buttress or locking plates.[5,6,9-11] However, due to the lack of anatomically contoured medial distal femoral plates in many trauma centers, surgeons frequently adapt implants originally intended for other regions, leading to intraoperative challenges such as improper fit, soft-tissue irritation, and suboptimal screw trajectory, creating a gap in standardized care.[6,7] The biomechanical consequences of these improvisations remain inadequately explored.

Moreover, although previous studies have examined general distal femur fixation strategies, there is a paucity of biomechanical investigations focused specifically on AO/OTA 33-B2.1 fracture patterns. In particular, the mechanical performance of screw-only constructs versus constructs supplemented by plates (standard or locking) under physiologically relevant cyclic and axial loading conditions remains unclear. To date, no biomechanical study has focused specifically on AO/OTA 33-B2.1 type medial condylar fractures. The rationale for conducting a biomechanical study on these fractures stems from their rarity, which has limited the availability of large clinical case series in the literature. As a result, clinical comparisons of treatment outcomes are nearly impossible.

In the present study, we hypothesized that the addition of a centrally positioned 6.5-mm cannulated screw or a medially contoured locking plate would significantly enhance axial stability compared to traditional three-screw constructs or screw-plate combinations. We, therefore, aimed to determine the construct which offers optimal fixation strength while maintaining surgical feasibility and minimizing implant burden.

MATERIALS AND METHODS

This single-center, experimental study was conducted at Ankara Bilkent City Hospital, Department of Orthopedics and Traumatology. The study used a total of 28 right synthetic femurs (Synbone AG, model 2200, Malans, Switzerland) of the same size and density (Figure 1). Ethics committee approval was not required, as this study involved biomechanical experiments conducted on synthetic bones.

The smooth geometry of the synthetic bone and the similarity of the bone structure minimize the variation between the specimens and provide a better standardization.[12] Cadaveric bone was not preferred in this study due to anatomical variations, differences in bone density, and the osteoporotic nature of most specimens.[13] Titanium 6.5-mm cannulated partial threaded screws (16-mm) were provided by Zimed™ Medical Co. (Zimed Medical Orthopedic Implant, Gaziantep, Türkiye). Titanium 3.5-mm plate and screws, 4.5-mm screws and 3.5/4.5 mm anterolateral proximal tibial anatomical locking plate were provided by Trauson Medical Instrument Company Limited (Trauson Medical Instrument Co. LTD, Changzhou, Jiangsu, China).

Fracture model

All fracture models were created by the same clinician according to the AO/OTA classification AO 33-B2.1 subtype. While creating the fracture models, the medial edge of the osteotomy line was designed to pass between the insertion site of the adductor magnus and the distal part of the vastus medialis origin as described in the study of Lee et al.[11]

A bristle saw was used to minimize bone loss in the osteotomy cuts. After fixing the synthetic models in a vise, a bristle saw was used to perform an oblique osteotomy, starting at the intercondylar

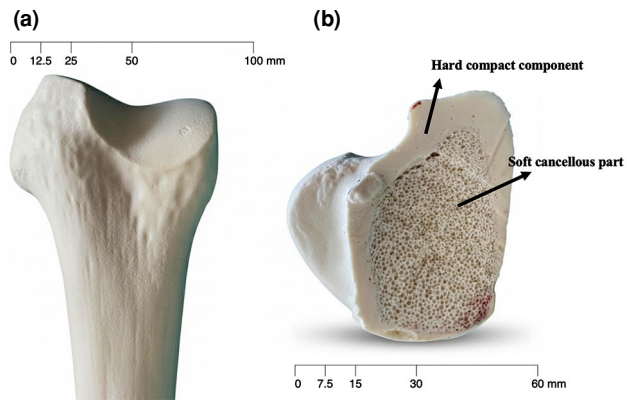

FIGURE 1. Synthetic distal femur model and internal structure. **(a)** Anterior view of the distal femur showing the smooth cortical surface of the medial condyle. **(b)** Coronal section of the same specimen demonstrating the hard compact component of the cortical shell and the underlying soft cancellous part, which reproduces the trabecular architecture of native bone. Scale bars indicate millimeters.

groove (The intersection point of the anatomical axis of the femur with the intercondylar groove was located 40 mm lateral to the medial condylar rim and 27 mm from the condylar rim), and ending 80 mm proximal to the distal medial condylar rim (60 mm proximal to the intercondylar groove), forming a 20° angle between the osteotomy line and the anatomical axis of the femur (Figure 2). To ensure reproducibility, we performed all cuts, and inter-specimen variation of the osteotomy angle was measured using a goniometer, which showed a variance of less than 3 ± 2.6°. Entry and exit points were measured from the anatomical landmarks (medial condylar rim and intercondylar notch) with a ruler and demonstrated a mean deviation of less than 2 mm. Verification was performed visually on synthetic femurs. Since the osteotomies were carried out on synthetic bones under direct visualization, no fluoroscopic imaging was deemed necessary. Before fixation, all fragments were anatomically reduced under direct view, and interfragmentary compression was achieved using tenaculum and

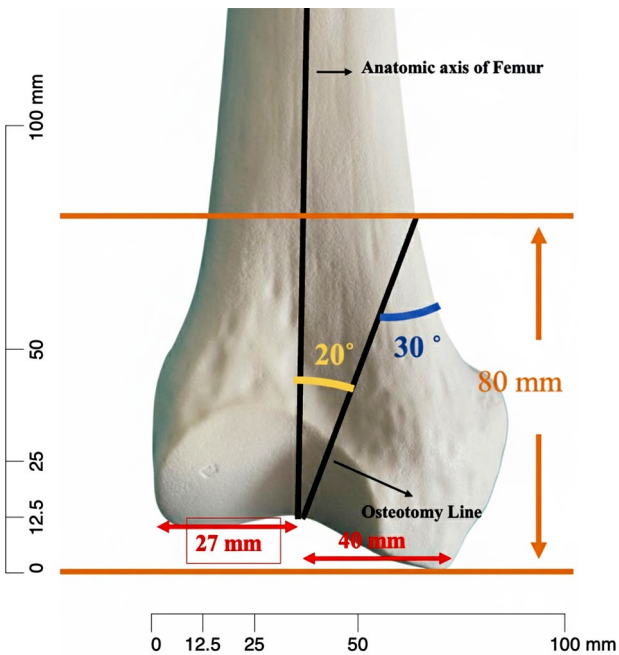

FIGURE 2. Preoperative osteotomy planning for the AO/OTA 33-B2.1 fracture model. Synthetic distal femur illustrating the planned oblique osteotomy (black line) used to reproduce a medial condyle fracture. The cut begins at the intercondylar groove and extends proximally with a 20° obliquity relative to the anatomic femoral axis. Key reference distances are indicated: 40 mm from the medial condylar rim to the osteotomy entry point, 27 mm from the lateral condylar rim to the anatomic axis, and 80 mm from the medial condylar rim to the proximal end of the osteotomy. The anatomic femoral axis is shown in black for orientation.

temporary Kirshner wires (K-wires) followed by lag screw insertion. The residual gap was confirmed to be < 1 mm in all cases.

Construct design

Seven constructs were created for each group (n = 28). After determining the entry and exit points on a pilot synthetic bone, screw placement was standardized using a tibial anterior cruciate ligament (ACL) drill guide and K-wires. The entry and exit coordinates, as well as the trajectories of all cannulated screws, are illustrated in Supplementary Figures 1-3. In Group 1, three 6.5-mm cannulated screws were inserted from the medial condyle to the lateral condyle of the femur, perpendicular to the fracture line and in a convergent manner to avoid the joint.[8] The first three cannulated screws were placed at equal intervals along the anterior and distal subchondral rim of the medial condyle in order to allow for standardized comparison of the biomechanical effects of the centrally positioned screw and the supplementary plates. We also hypothesized that positioning the screws in the subchondral region would enhance construct stability, given the superior bone quality and increased resistance to displacement in this area. In Group 2, an additional 6.5-mm lag screw was inserted in the center of the condyle in addition to the screw combination in Group 1. In Group 3, three 6.5-mm cannulated screws and a 3.5-mm buttress plate were used. In Group 4, in addition to three cancellous cannulated screws, the anterolateral proximal tibial locking plate was used.

For Group 1, fixation was performed using two 6.5 × 75 mm and one 6.5 × 70 mm partially threaded (16-mm thread) cannulated screws. Screws were advanced with a cannulated screwdriver under manual control until the manufacturer's recommended torque resistance was encountered; no torque-limiting device was available. This standardized method was consistently applied across all specimens. In Group 2, an additional 6.5 × 85 mm partially threaded (16-mm thread) cannulated screw was inserted centrally. Washers were not used in any specimen. Screw lengths were selected to ensure bicortical purchase in the far fragment.

In Group 3, fixation included the screws described in Group 1 plus a buttress plate. The most proximal two holes of the plate were filled with 3.5 × 40 mm and 3.5 × 42 mm locking screws, each inserted using a torque-limiting driver set to

1.5 Nm. The third proximal hole was filled with a 4.5 mm cortical screw, which was tightened without a torque limiter and advanced manually until firm resistance was achieved.

In Group 4, the screws from Group 1 were supplemented with a reversed proximal tibial locking plate. Three proximal locking screws (5 × 40 mm, 5 × 44 mm, and 5 × 46 mm) were inserted using a 4 Nm torque-limiting screwdriver. Distally, five locking screws were applied: proximal 3.5 × 65 mm, middle-anterior 3.5 × 65 mm, middle-posterior 3.5 × 70 mm, distal-anterior 3.5 × 70 mm, and distal-posterior 3.5 × 70 mm. All distal screws were tightened with a 1.5 Nm torque-limiting screwdriver.

Group 1

The entry point for the first 6.5-mm cannulated screw was identified as 1 cm superior to the Blumensaat line and 1 cm proximal to the distal end of the medial condyle in the sagittal plane. This point also intersects the anatomical axis of the femur in the sagittal plane. The entry points for the second and third 6.5-mm cannulated screws were, then, determined at 1 cm intervals on the periphery of the condyle and superior to the Blumensaat line (Figure 3). To ensure standardization, cannulated screws were inserted from the same designated entry points in all groups. After temporary fixation achieved with a bone clamp and K-wires using the ACL reconstruction drill guide, 6.5-mm partially threaded (16 mm) cannulated screw fixation was performed at the described points (Figure 3). Final fixation in the load cell for all groups is shown in Figure 4.

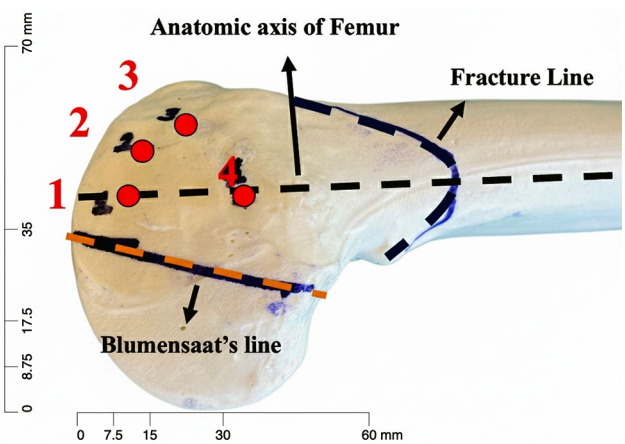

FIGURE 3. Entry points for 6.5 mm cannulated lag screws. Anterior view of the medial distal femur showing the standardized screw entry coordinates used for Groups 1-4. Red circles (1-4) indicate the designated starting points for the three primary subchondral screws and the optional central fourth screw. The fracture line and the Blumensaat's line are marked for reference, and the anatomic axis of the femur is indicated by the vertical black arrow.

Group 2

After the bone models were fixed as described in Group 1, an additional fourth screw fixation was applied at the point where it intersected the anatomical axis of the femur in the sagittal plane 2 cm proximal to the first screw entry point (Figure 3). This point corresponds to the center of the medial condyle of the femur.

Group 3

After fracture reduction performed with a bone clamp and temporary K-wires, a slightly pre-contoured 6-hole 3.5-mm locking plate was fixed to the bone in anti-glide mode using a 3.5-mm cortical screw and locking screws in the proximal part of the plate, followed by fixation with three 6.5-mm cannulated partially threaded (16 mm) screws as described in Group 1. To minimize implant lift-off, plates were contoured before application and clamped to the medial condyle during fixation. Offset was measured with a caliper at multiple points, and in all cases remained < 1 mm. The plate fitting parameters are shown in Supplementary Figure 4.

Group 4

After fixation with 6.5-mm cannulated screws as described in Group 1, a 5-hole 3.5/4.5-mm ipsilateral anterolateral proximal tibial anatomical locking plate (Trauson Medical Instrument Co. Ltd, Changzhou, Jiangsu, China) was reversed and placed to fit the medial condyle and fixation was completed. The plate fitting parameters are shown in Supplementary Figure 5. Screw holes, which indicated with red dots, could not be used due to joint penetration risk (Figure 5).

Mechanical testing and loading protocol

The biomechanical tests of the study were carried out at the Biomechanics Laboratory at TOBB University of Economics and Technology University, Department of Mechanical Engineering.

After osteotomy and instrumentation, the proximal portion of the specimens was placed in a custom-made polyurethane mold and placed in the 2015EMY01 axial compression device (Capacity: 20 kN-10 Hz, Labiotech, Ankara, Türkiye) to apply axial loading to the medial femoral condyle. Specimens were potted with the

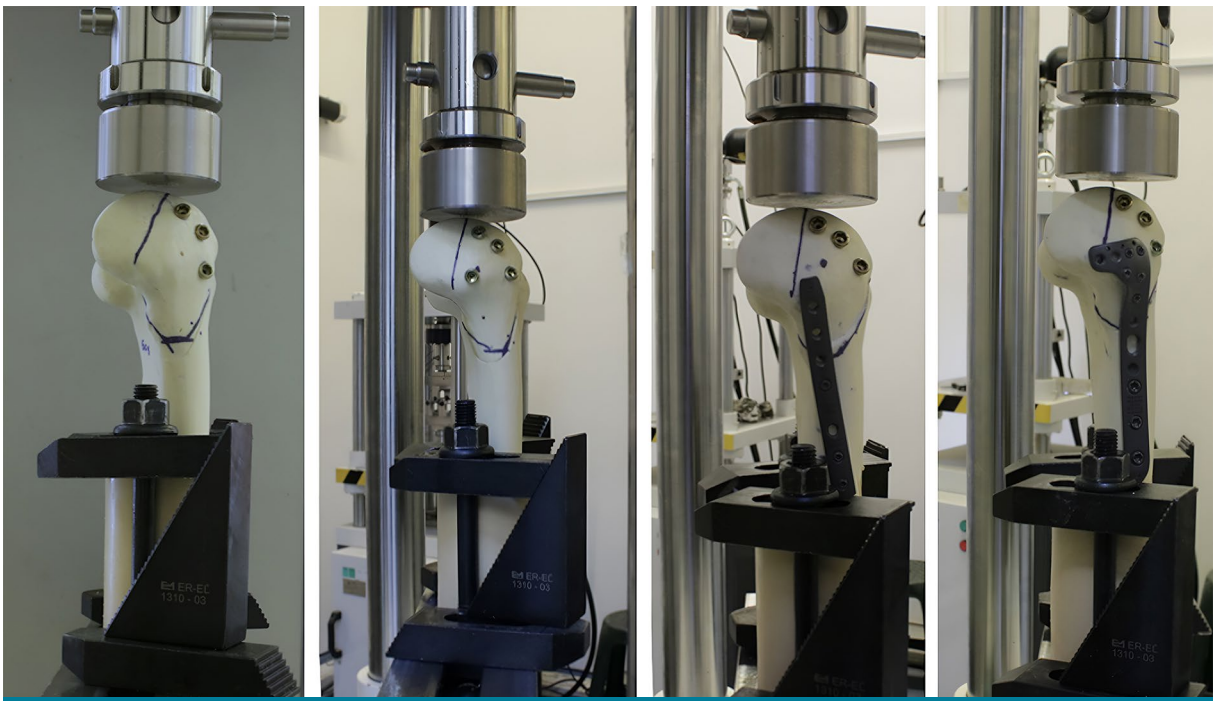

FIGURE 4. Final construct fixation in the axial loading test system. Representative photographs of the synthetic distal femur specimens mounted in the servo-hydraulic testing machine for axial loading. The constructs are secured in custom poly-urethane pots with the femoral shaft aligned vertically and the medial condyle positioned beneath the flat loading platen. Different images illustrate the screw-only and plate-augmented configurations under identical boundary conditions.

femoral anatomical axis oriented vertically and perpendicular to the load cell, with the distal condyles positioned in 5° of valgus relative to the mechanical axis to reproduce physiological joint-line obliquity. The medial condyle was oriented at 0° of flexion and 0° of axial rotation, verified with a digital goniometer. Axial loading was applied through a custom cylindrical polyethylene indenter (25 mm in diameter, flat contact surface) that distributed the load evenly across the medial condyle. The contact interface was left unconstrained in varus-valgus and anteroposterior translation, allowing pure axial loading without artificial shear restriction. The fixture compliance was measured before testing and found to be negligible (< 0.1 mm displacement at 1 kN). A schematic illustrating the specimen coordinates, potting angle, and load application footprint is provided in Figure 6. Fracture displacement was quantified from the actuator cross-head travel recorded by the testing machine after correction for system compliance; A high-resolution camera (EOS 750D, Canon®, Tokyo, Japan) placed 120 cm away from the fracture line was used for digital image correlation (DIC).

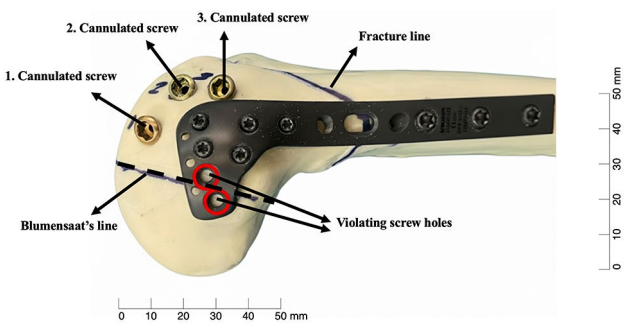

FIGURE 5. Application of the anatomical proximal tibial locking plate (Group 4). Lateral view of the medial distal femur demonstrating placement of the reversed anterolateral proximal tibial locking plate combined with three cannulated lag screws (1-3) across the fracture line. Red circles highlight the distal plate holes that were intentionally left unused because screw insertion at these positions would risk intra-articular penetration along the Blumensaat's line.

The specimens were first subjected to dynamic testing. The specimens were subjected to a preload of 100 N at 2 mm/min prior to dynamic loading. The system was, then, loaded to 300 N at 10 mm/min and then tested under dynamic loading conditions at a frequency of 4 Hz between 200 N and 600 N for 10,000 cycles, as described in the studies by

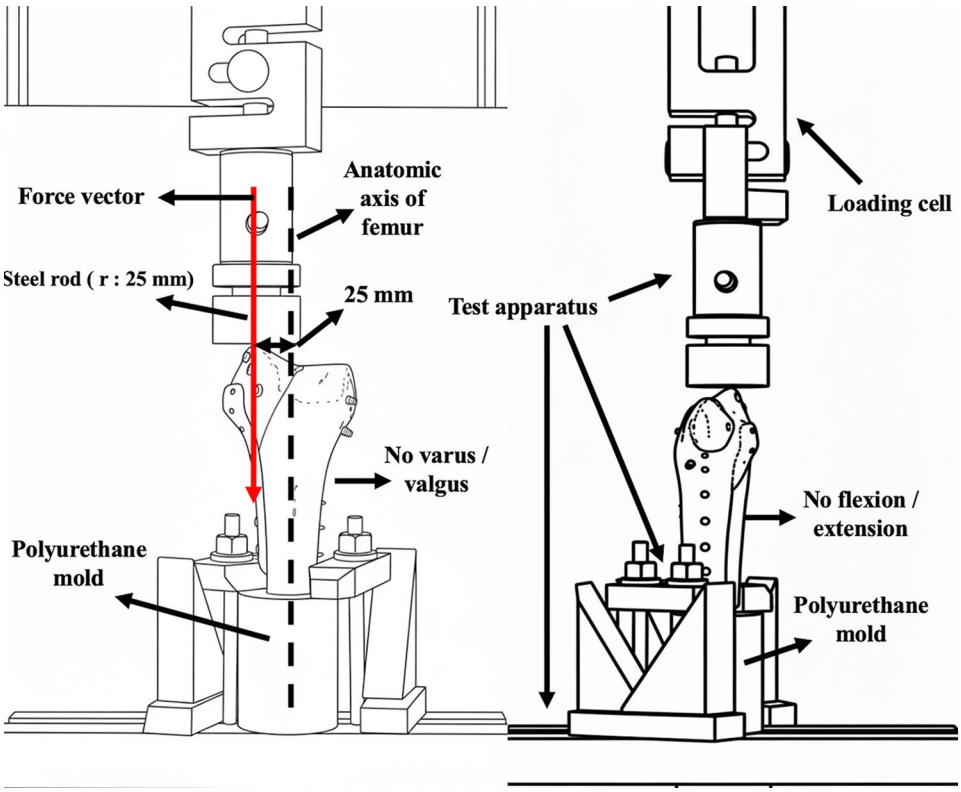

FIGURE 6 Diagram illustrating the custom fixture used for biomechanical testing. Synthetic femurs were embedded in polyurethane molds with the anatomic femoral axis aligned vertically beneath the loading cell. A 25-mm radius steel rod applied the force vector perpendicular to the condylar surface. The apparatus constrained the specimen to prevent varus/valgus angulation and flexion/extension, ensuring pure axial loading while allowing measurement of displacement across the fracture site.

Jarit et al.[14] and Yao et al.[15] The stiffness of the specimens was calculated from the slope of the load-displacement curve obtained, when the system was loaded from 100 N to 300 N prior to dynamic loading. During the tests, the displacement data from the load cell at 100 and 10,000 cycles were used to calculate the displacement of the fracture line on the vertical axis. After the dynamic loading, static loading was applied at a speed of 10 mm/min until fracture occurred in the system (catastrophic failure) (Figure 7).[15,16] Displacement values were recorded during loading and the maximum load values of the specimens were obtained from the load-displacement graph. Given the importance of articular congruity in these fractures, load values at 1 mm, 2 mm and 3 mm of displacement (articular step-off) were specifically measured and interpreted as indicators of fixation failure.[8]

Displacement thresholds of 1, 2, and 3 mm were selected in accordance with prior biomechanical

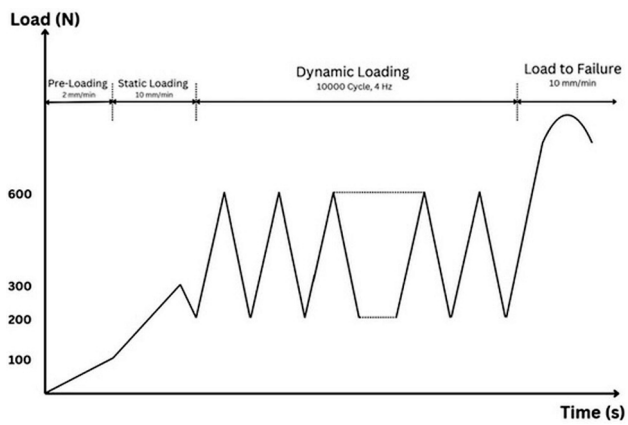

FIGURE 7. Loading protocol used for biomechanical testing. Schematic representation of the sequential loading regimen applied to each specimen. After an initial pre-loading phase (2 mm/min) to seat the construct, specimens underwent static loading at 10 mm/min followed by dynamic cyclic loading of 10,000 cycles at 4 Hz between 200 N and 600 N. Finally, a monotonic load-to-failure test was performed at 10 mm/min until catastrophic displacement or construct failure occurred.

studies of distal femoral condyle and Hoffa fractures, where these cut-offs are frequently reported as functional failure criteria.[13,15,17] In particular, a displacement of 2 mm has been widely adopted as the most clinically relevant threshold, since articular incongruities beyond this level are associated with poor joint mechanics. Load values at these thresholds were recorded directly from the testing machine's displacement transducer during monotonic static loading and, therefore, represent instantaneous displacement under load. Residual deformation was assessed separately in the cyclic protocol by calculating the difference in vertical displacement between the 100th and 10,000th loading cycles.

Statistical analysis

Study power analysis and sample size calculation were performed using the G*Power version 3.1.9.7 software (Heinrich Heine University Düsseldorf, Düsseldorf, Germany). By using the mean and standard deviation of the results, the effect size of the study was utilized. The sample size for each group was seven and the error probability was chosen as 0.05. As a result, the power of the study was calculated as 0.99 which was enough proof to decide the sample size was sufficient.

Statistical analysis was performed using the IBM SPSS version 27.0 software (IBM Corp., Armonk, NY, USA). Normality was assessed using the Shapiro-Wilk test, and homogeneity of variances was evaluated with Levene's test. Descriptive data were expressed in mean ± standard deviation (SD), median (min-max) or number and frequency, where applicable. For variables where the assumption of normality was violated, non-parametric analyses were conducted. In this case, Kruskal-Wallis test was used to detect overall group differences, followed by Bonferroni-adjusted pairwise comparisons to identify specific group contrasts. A p value of < 0.05 was considered statistically significant.

RESULTS

Dynamic tests

The mean stiffness values of the groups were 300 ± 80 N/mm, 411 ± 94 N/mm, 650 ± 110 N/mm, and 802 ± 70 N/mm. There was a statistically significant difference between Group 1 and Group 2 and between Group 1 and Group 4.

The displacement of the load cell during the dynamic tests was calculated by considering the difference between the data taken at 10,000th and 100th cycles (Table I). There was a statistically significant difference between Group 1 and Group 4 and between Group 2 and Group 4 (Table II).

Static tests

The mean values of the maximum axial load values obtained at the end of the static loading tests. Group 1 withstood less load than the other groups (1455 ± 228 N) and Group 4 withstood more load than the other groups (2360 ± 389 N) (Table I). There was a statistically significant difference between Group 4 and Group 1 (p = 0.001) and between Group 1 and Group 2 (p = 0.016) in terms of maximum loading. There was no significant difference between Group 4 and Group 2 (Table II), which could be attributed to the fact that the central screw added in Group 2 significantly increased stability.

TABLE I
Mean and standard deviation of results

	Group 1	Group 2	Group 3	Group 4
	Mean ± SD	Mean ± SD	Mean ± SD	Mean ± SD
Maximum load (N)	1454.71 ± 228.01	2112.33 ± 190.43	1903.86 ± 214.75	2360.43 ± 389.31
Stiffness (N/mm)	300.37 ± 79.98	411.06 ± 93.73	650.08 ± 110.03	802.20 ± 69.84
Load at 1 mm (N)	335.86 ± 69.20	396.67 ± 59.48	461.17 ± 24.40	616.67 ± 15.34
Load at 2 mm (N)	597.29 ± 142.43	747.50 ± 155.93	754.33 ± 37.88	1138.50 ± 86.82
Load at 3 mm (N)	849.86 ± 245.45	1040.83 ± 202.32	1063.00 ± 65.23	1582.50 ± 159.81
Displacement at 100th cycles (mm)	2.39 ± 0.77	1.69 ± 0.67	1.57 ± 0.08	1.01 ± 0.09
Displacement at 10,000th cycles (mm)	2.63 ± 0.82	1.90 ± 0.62	1.74 ± 0.18	1.13 ± 0.13
Difference between 100th 10,000th cycles (mm)	0.24 ± 0.18	0.21 ± 0.22	0.16 ± 0.11	0.13 ± 0.04

SD, standard deviation.

TABLE II
Statistical comparison of the groups

Compared groups	Group 1 *vs.* Group 2	Group 1 *vs.* Group 3	Group 1 *vs.* Group 4	Group 2 *vs.* Group 3	Group 2 *vs.* Group 4	Group 3 *vs.* Group 4
Maximum load (N)	0.016*	0.282	0.001*	1.000	1.000	0.446
Stiffness (N/mm)	1.000	0.016*	0.001*	0.377	0.012*	1.000
Load at 1 mm (N)	1.000	0.103	0.001*	1.000	0.017*	0.550
Load at 2 mm (N)	1.000	0.775	0.001*	1.000	0.072	0.112
Load at 3 mm (N)	1.000	1.000	0.001*	1.000	0.065	0.081
Displacement at 100th cycles (mm)	1.000	0.698	0.001*	1.000	0.112	0.130
Displacement at 10,000th cycles (mm)	1.000	0.801	0.001*	1.000	0.072	0.077
Difference between 100th 10,000th cycles (mm)	1.000	0.103	0.001*	1.000	0.017*	0.550

* Statistically significant.

For all groups, the load values with the load cell displaced by 2 mm were determined (Table I). The mean load value of Group 1 was lower than the other groups (597 ± 133 N). In addition, a displacement of 2 mm was observed during dynamic loading. In the other groups, 2-mm displacement was observed after the dynamic test. In the Group 4, 2 mm of displacement was observed at higher loads than the other groups (1138 ± 87 N) (Table II).

Failure modes were systematically classified as follows: (1) screw pullout or cut-out from the subchondral bone, (2) plate bending or deformation, (3) condylar fragment split or subsidence, intra-articular joint penetration of screws, (4) proximal periprosthetic fractures, and (5) potting block failure. The most frequent failure mechanism in screw-only groups (Groups 1 and 2) was articular subsidence with screw cut-out, whereas the addition of a buttress plate (Group 3) reduced screw migration, but occasionally resulted in plate bending and condylar split fractures. In the locking plate group (Group 4), proximal periprosthetic fractures were observed, consistent with a stress-riser effect at the end of the construct. Representative images of these patterns are presented in Figure 8.

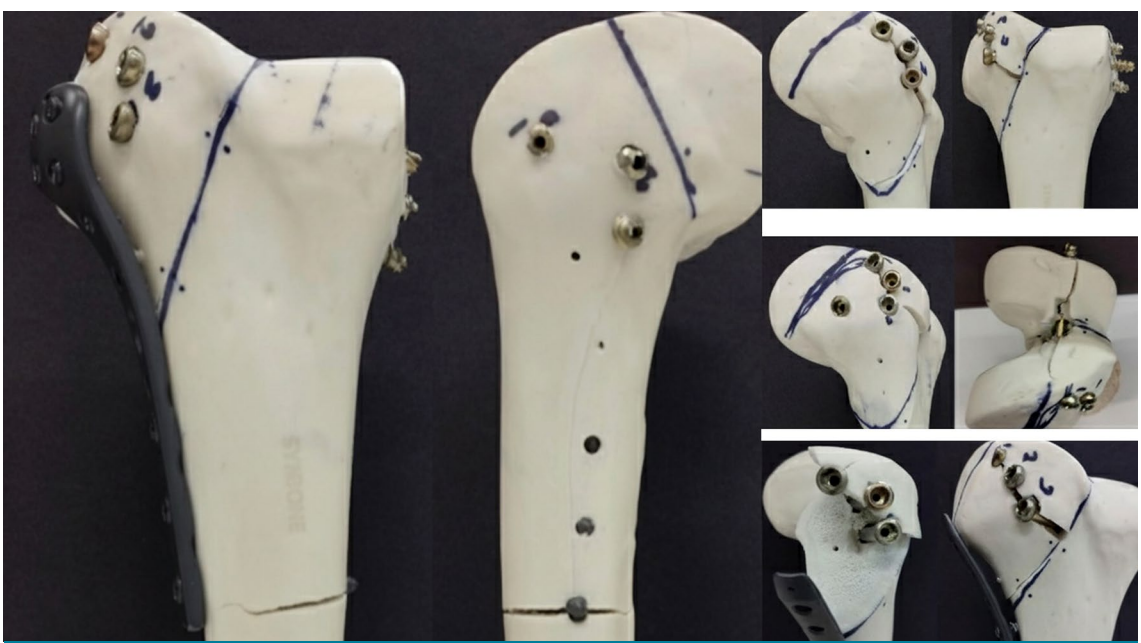

FIGURE 8. Representative failure modes observed during axial loading tests.

DISCUSSION

In the present biomechanical study, we attempted to identify the most stable construct (in terms of rigidity, maximum load to failure and load at 2-mm displacement) for the fixation of medial femoral condyle fractures, using synthetic femurs to standardize bone quality and minimize confounding variability. The most critical findings are as follows: (1) Construct stiffness was highest in Group 4, where a reversed anatomical proximal tibial locking plate was combined with three 6.5-mm cannulated screws. This group also demonstrated the highest load to failure and resistance to 2-mm displacement. (2) Addition of a centrally placed fourth screw (Group 2) led to significant improvements in load-bearing capacity compared to the traditional three-screw construct (Group 1), but not to the same extent as the locking plate construct. (3) The buttress plate group (Group 3) showed increased stiffness over the screw-only groups, but did not significantly outperform Group 2 in load at 2-mm displacement or in maximum load capacity. The results are consistent with the work of Khalafi et al.,[8] who reported increased stability with centrally placed 6.5-mm screws in unicondylar fractures. Our data supports the notion that screw trajectory and position, particularly central placement aligned with the anatomic axis, have a major influence on overall construct performance. Additionally, stability of interfragmentary screws is closely related to their pull-out strength, which is influenced by factors such as outer diameter, thread geometry, and implant material.[18] Larger diameter screws usually provide greater pull-out strength.[8] Therefore, we selected 6.5-mm cannulated, partially threaded screws for interfragmentary compression, consistent with previous recommendations.[8,19] Notably, the central screw (Group 2) increased axial stiffness by 37% and load capacity by 45% compared to the three-screw configuration, highlighting its biomechanical relevance. Although some authors have advocated two-screw fixation constructs in the treatment of unicondylar femoral fractures, we believe such configurations may be insufficient to support early mobilization and weight-bearing.[8,17,19-21] This concern is largely based on the fact that existing clinical data in the literature are both outdated and limited, and most biomechanical studies on unicondylar fractures have primarily focused on static loading rather than dynamic testing conditions. According to Becker et al.[22] and several other authors,[23-25] peak femorotibial contact forces could reach up to 261% of body weight during walking, 346% during stair descent, and as high as 550% in instances of sudden loss of balance. In our study, a 2-mm articular step-off was defined as a threshold for fixation failure. The loads corresponding to this displacement were 597 N, 748 N, 754 N, and 1138 N for Groups 1 through 4, respectively. Notably, only Group 4 exceeded the approximate load exerted by a healthy 70-kg individual during single-leg stance. While this comparison does not fully replicate *in vivo* conditions, it may offer clinicians a practical perspective on the relative strength and clinical utility of each construct. Tibiofemoral contact forces vary substantially with activity, reaching ~2-3 × body weight during level walking and 3-5 × body weight during stair descent or sudden imbalance.[22,23] Therefore, our 2-mm data should be considered relative benchmarks of construct performance under axial compression rather than direct predictors of safe postoperative loading. While stair descent can produce higher peak forces, our cyclic protocol most closely reproduces the repetitive loads encountered during early protected weight-bearing.

Interestingly, although Group 3 (buttress plate) had higher stiffness than Group 2, the loading performance at critical displacement thresholds (1 mm and 2 mm) was comparable, suggesting that the fourth screw may substitute for the buttress plate in select cases. In most biomechanical studies, stability is considered to correlate positively with construct stiffness.[26] It is usually accepted that a more rigid construct would allow less motion at the fracture site. However, this assumption does not hold true in every clinical or mechanical scenario.[17] This observation highlights the distinction between construct stiffness and overall mechanical strength. While stiffness (measured in N/mm) reflects the elastic response during initial loading, it does not necessarily correlate with failure resistance or load tolerance at clinically relevant displacement thresholds. Constructs with lower stiffness may allow for a more gradual energy dissipation and improved load distribution, particularly under dynamic or repetitive loading conditions.[27] This can prevent localized stress concentrations and delay catastrophic failure, thereby enhancing overall load-bearing capacity. Therefore, the superior performance of the less rigid construct in our study can be attributed to the interaction between screw trajectory, bone-implant interface dynamics, and the capacity of the construct to redistribute loads over time. These findings underscore the importance of considering both stiffness and ultimate strength

while evaluating biomechanical fixation strategies for intra-articular fractures. This finding has meaningful clinical implications for minimally invasive strategies, particularly in osteoporotic bone where screw purchase may be limited.[28] However, in osteoporotic bone or in fractures with metaphyseal comminution, a buttress plate may still be preferred when additional anti-glide stability is required.

Superior performance observed in Group 4 validates the use of a locking plate in high-demand cases. However, the absence of plates specifically designed for the medial femoral condyle remains a barrier. Intraoperatively, surgeons often must adapt existing plates, leading to prolonged operative times due to contouring and positioning challenges. Despite encountering anatomical fit challenges while using the medial distal femoral TomoFix® plate (J&J MedTech, NJ, USA) in combination with a lag screw for the treatment of AO/OTA 33B2.1 fractures in elderly patients, Lee et al.[11] reported superior clinical outcomes with this construct. Our experience aligns with Upadhyay et al.,[7] who showed that anterolateral proximal tibial plates offer the best contour fit when reversed for the medial femur. Surgeons should nonetheless be aware of potential technical challenges such as soft-tissue irritation or the need for careful contouring when using a reversed tibial plate on the medial femur.

Our rationale to use this plate on the medial distal femur is grounded in three key advantages highlighted in the literature: (1) its close anatomical conformity to the medial metaphyseal flare, which minimizes notch penetration risk and allows safe placement of multiple distal locking screws;[7,29] (2) its ability to provide a broad buttress/antiglide surface that enhances biomechanical stability against varus collapse and shear along the oblique fracture plane;[30] and (3) its capacity to accommodate a convergent-divergent distal screw configuration that forms a subchondral "rafting" construct beneath the articular surface, thereby improving resistance to articular displacement.[29] In addition, recent case reports describing successful clinical applications of the reversed anterolateral proximal tibial plate further supported our decision to select this implant for the present study.[6,31-34] Collectively, these attributes position the reversed anterolateral proximal tibial plate as a practical and mechanically robust implant choice for AO/OTA 33-B2.1 fractures, and a postoperative radiograph of the construct is shown in Figure 9. Despite anatomical adaptation, plate application in Group 4 allowed for five distal screws without intra-articular penetration, preserving fixation strength.

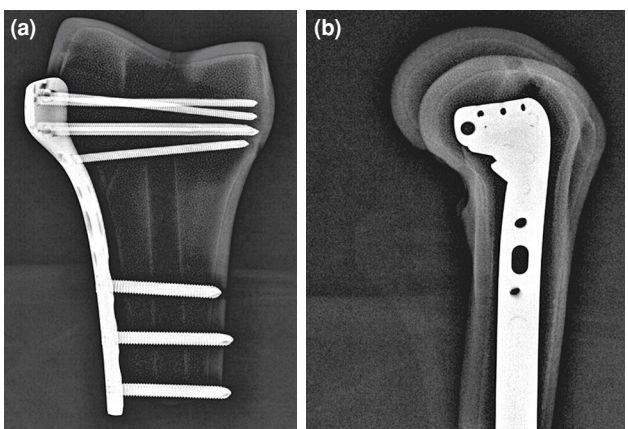

FIGURE 9. Postoperative radiograph of the reversed anterolateral proximal tibial locking plate construct. **(a)** Anteroposterior and **(b)** lateral radiographs of a specimen fixed with a reversed anterolateral proximal tibial locking plate. The images demonstrate accurate plate contouring to the medial distal femur, safe screw trajectories beneath the subchondral surface, and absence of joint penetration.

Considering clinical implications, for patients with good bone quality and minimal comminution, central screw addition (Group 2) offers a soft tissue-sparing, cost-effective alternative. However, in osteoporotic bone or in fractures with metaphyseal comminution, a buttress plate may still be preferred when additional anti-glide stability is required. Buttress plating (Group 3) may be preferred, when additional anti-glide stability is needed, particularly in osteoporotic bone. Anatomic locking plates (Group 4) should be considered in elderly patients or in fracture configurations at high risk of displacement, although the need for intraoperative plate contouring may increase surgical time.

Nonetheless, this study has several limitations. First, it does not fully replicate clinical conditions, as it excludes the influence of soft tissue tension and muscle-tendon dynamics on fracture alignment and stabilization.[13,35] Second, the use of synthetic bone models lacks the anisotropy and variability present in human bone. Third, only axial loading was applied. While clinically relevant to early weight-bearing, axial compression does not reproduce the complex, multidirectional stresses experienced by the distal femur *in vivo*. The medial condyle is subjected to torsional

stresses, varus-valgus bending moments, and shear forces, particularly during activities such as pivoting, stair climbing, or rising from a chair. These loading conditions may induce different failure mechanisms than those seen under axial compression. To illustrate, screw-based constructs may be more vulnerable to torsional loosening or shear cut-out, whereas plate-based constructs may better resist torsion and bending but deform earlier under direct axial load. Furthermore, our loading protocol applied force at a single point on the condylar surface, which represents only one clinical scenario. *In vivo*, load transmission occurs across a variable contact area that shifts with knee flexion and is influenced by soft tissues. The absence of simulated muscle forces, ligamentous tension, and joint kinematics may therefore bias construct rankings. Finally, specimens were subjected to only 10,000 cycles; given that patients typically perform approximately 5,000 cycles per day, further studies incorporating higher cycle counts and multiaxial loading are warranted.[14,36] Further studies with larger sample groups and extended dynamic cyclic loading protocols (e.g., 50,000 or 100,000 cycles) are warranted. Moreover, biomechanical models that incorporate knee kinematics (such as gait cycles) and evaluate the effects of multi-axial forces on fracture stability would provide more comprehensive insights. In addition, assessing the response of different fixation methods under axial loading, bending, torsion, and varus-valgus stresses may better inform clinicians in determining the most effective construct.

In conclusion, in the treatment of medial femoral condyle fractures, the central placement of a cannulated screw enhanced axial stability and represented a less invasive alternative to buttress plating under the conditions of this synthetic model. The strongest construct was observed with the combination of cannulated screws and an anatomical locking plate. These findings are limited to axial loading and the tested endpoints; therefore, further biomechanical investigations under multi-axial conditions, as well as cadaveric and clinical studies, are required before generalizing to early weight-bearing. The choice of fixation method for optimal stabilization should still be considered a matter of the surgeon's preference and experience. The development of anatomically contoured locking plates specifically designed for the medial condyle remains an important direction for future implant design and validation.

Data Sharing Statement: The data that support the findings of this study are available from the corresponding author upon reasonable request.

Author Contributions: A.D.: Study design and main writer of the work; E.K.: Study design, material preparation and implantation; E.N.P.: Statistical analysis; F.K.E.E.: Biomechanical testing of materials, designed biomechanical protocols, interpretation of the data; T.K.: Data collection and statistical analysis; B.K.: Proof-reading, implantation of the materials; G.O.: Mentor of the work, proof-reading; O.B.: Study design, editing the manuscript; T.D.: Setup of the testing machine, guidance.

Conflict of Interest: The authors declared no conflicts of interest with respect to the authorship and/or publication of this article.

Funding: The authors received no financial support for the research and/or authorship of this article.

AI Disclosure: The authors declare that artificial intelligence (AI) tools were not used, or were used solely for language editing, and had no role in data analysis, interpretation, or the formulation of conclusions. All scientific content, data interpretation, and conclusions are the sole responsibility of the authors. The authors further confirm that AI tools were not used to generate, fabricate, or 'hallucinate' references, and that all references have been carefully verified for accuracy.

REFERENCES

1. Gwathmey FW Jr, Jones-Quaidoo SM, Kahler D, Hurwitz S, Cui Q. Distal femoral fractures: Current concepts. J Am Acad Orthop Surg 2010;18:597-607. doi: 10.5435/00124635-201010000-00003.
2. Manfredini M, Gildone A, Ferrante R, Bernasconi S, Massari L. Unicondylar femoral fractures: Therapeutic strategy and long-term results. A review of 23 patients. Acta Orthop Belg 2001;67:132-8.
3. Kolmert L, Wulff K. Epidemiology and treatment of distal femoral fractures in adults. Acta Orthop Scand 1982;53:957-62. doi: 10.3109/17453678208992855.
4. Trillat A, Dejour H, Bost J, Nourissat C. Unicondylar fractures of the femur. Rev Chir Orthop Reparatrice Appar Mot 1975;61:611-26. French.
5. Gangavalli AK, Nwachuku CO. Management of distal femur fractures in adults: An overview of options. Orthop Clin North Am 2016;47:85-96. doi: 10.1016/j.ocl.2015.08.011.
6. Kodama H, Saku I, Tomoyama S. Surgical treatment of femoral medial condyle fracture with lag screws and proximal tibial plate: A case report. Int J Surg Case Rep 2020;70:101-5. doi: 10.1016/j.ijscr.2020.04.060.
7. Upadhyay P, Syed F, Ramoutar DN, Ward J. The missing piece of the trauma armoury-medial femoral condyle plate. Injury 2022;53:1237-40. doi: 10.1016/j.injury.2021.11.034.
8. Khalafi A, Hazelwood S, Curtiss S, Wolinsky P. Fixation of the femoral condyles: A mechanical comparison of small and large fragment screw fixation. J Trauma 2008;64:740-4. doi: 10.1097/TA.0b013e318165c12a.
9. Bel JC, Court C, Cogan A, Chantelot C, Piétu G, Vandenbussche E, et al. Unicondylar fractures of the distal femur. Orthop Traumatol Surg Res 2014;100:873-7. doi: 10.1016/j.otsr.2014.10.005.

10. Ehlinger M, Ducrot G, Adam P, Bonnomet F. Distal femur fractures. Surgical techniques and a review of the literature. Orthop Traumatol Surg Res 2013;99:353-60. doi: 10.1016/j.otsr.2012.10.014.
11. Lee HH, Kim WY, Kim YW, Kim KJ, Lee SW. Characteristics of medial condyle sagittal fracture of distal femur involving intercondylar notch in geriatric patients. Arch Orthop Trauma Surg 2020;140:1687-93. doi: 10.1007/s00402-020-03406-6.
12. Zhang W, Luo CF, Putnis S, Sun H, Zeng ZM, Zeng BF. Biomechanical analysis of four different fixations for the posterolateral shearing tibial plateau fracture. Knee 2012;19:94-8. doi: 10.1016/j.knee.2011.02.004.
13. Sun H, He QF, Huang YG, Pan JF, Luo CF, Chai YM. Plate fixation for Letenneur type I Hoffa fracture: A biomechanical study. Injury 2017;48:1492-8. doi: 10.1016/j.injury.2017.03.044.
14. Jarit GJ, Kummer FJ, Gibber MJ, Egol KA. A mechanical evaluation of two fixation methods using cancellous screws for coronal fractures of the lateral condyle of the distal femur (OTA type 33B). J Orthop Trauma 2006;20:273-6. doi: 10.1097/00005131-200604000-00007.
15. Yao SH, Su WR, Hsu KL, Chen Y, Hong CK, Kuan FC. A biomechanical comparison of two screw fixation methods in a Letenneur type I Hoffa fracture. BMC Musculoskelet Disord 2020;21:497. doi: 10.1186/s12891-020-03527-4.
16. Khalafi A, Curtiss S, Hazelwood S, Wolinsky P. The effect of plate rotation on the stiffness of femoral LISS: A mechanical study. J Orthop Trauma 2006;20:542-6. doi: 10.1097/01.bot.0000244996.45127.ad.
17. Hak DJ, Nguyen J, Curtiss S, Hazelwood S. Coronal fractures of the distal femoral condyle: A biomechanical evaluation of four internal fixation constructs. Injury 2005;36:1103-6. doi: 10.1016/j.injury.2005.02.013.
18. Leggon R, Lindsey RW, Doherty BJ, Alexander J, Noble P. The holding strength of cannulated screws compared with solid core screws in cortical and cancellous bone. J Orthop Trauma 1993;7:450-7. doi: 10.1097/00005131-199310000-00008.
19. Ostermann PA, Hahn M, Ekkernkamp A, Neumann K, Muhr G. Monocondylar fractures of the femur. Therapeutic strategy and clinical outcome. Chirurg 1997;68:72-6. doi: 10.1007/s001040050153.
20. Stover M. Distal femoral fractures: Current treatment, results and problems. Injury 2001;32:SC3-13. doi: 10.1016/s0020-1383(01)00179-6.
21. Siliski JM, Mahring M, Hofer HP. Supracondylar-intercondylar fractures of the femur. Treatment by internal fixation. J Bone Joint Surg Am 1989;71:95-104.
22. Becker R, Kopf S, Karlsson J. Loading conditions of the knee: What does it mean? Knee Surg Sports Traumatol Arthrosc 2013;21:2659-60. doi: 10.1007/s00167-013-2741-3.
23. Sasaki K, Neptune RR. Individual muscle contributions to the axial knee joint contact force during normal walking. J Biomech 2010;43:2780-4. doi: 10.1016/j.jbiomech.2010.06.011.
24. Taylor WR, Heller MO, Bergmann G, Duda GN. Tibio-femoral loading during human gait and stair climbing. J Orthop Res 2004;22:625-32. doi: 10.1016/j.orthres.2003.09.003.
25. Morrison JB. The mechanics of the knee joint in relation to normal walking. J Biomech 1970;3:51-61. doi: 10.1016/0021-9290(70)90050-3.
26. Wilkens KJ, Curtiss S, Lee MA. Polyaxial locking plate fixation in distal femur fractures: A biomechanical comparison. J Orthop Trauma 2008;22:624-8. doi: 10.1097/BOT.0b013e31818896b3.
27. Bottlang M, Doornink J, Fitzpatrick DC, Madey SM. Far cortical locking can reduce stiffness of locked plating constructs while retaining construct strength. J Bone Joint Surg Am 2009;91:1985-94. doi: 10.2106/JBJS.H.01038.
28. Kalem M, Baltacı Ç, Açar Hİ, Uslan Y, Perdeci EN, Şahin E. Biomechanical evaluation of fixation techniques for posteromedial tibial plateau fractures: A cadaveric model. Jt Dis Relat Surg 2025;36:620-9. doi: 10.52312/jdrs.2025.2373.
29. Leung F, Fang CX, Yung CSY, Leung FKL. Determination of the ideal plate for medial femoral condyle fracture fixation: An anatomical fit and biomechanical study. BMC Musculoskelet Disord 2024;25:296. doi: 10.1186/s12891-024-07374-5.
30. Dehoust J, Hinz N, Münch M, Behnk F, Kowald B, Schulz AP, et al. Biomechanical comparison of different double plate constructs for distal supracondylar comminuted femur fractures (AO/OTA 33-A3). Injury 2025;56:112324. doi: 10.1016/j.injury.2025.112324.
31. Liu ZH, Wang T, Fang C, Wong TM, Lin LL, Wang X, et al. Reverse contralateral proximal tibial plating and cannulated screws fixation for Hoffa fracture: A case report. Trauma Case Rep 2021;32:100443. doi: 10.1016/j.tcr.2021.100443.
32. Chen YC, Lin CH. Surgical treatment of femoral medial condyle impaction fracture complicated with Hoffa fragment by contralateral medial distal tibia plate: A case report. BMC Musculoskelet Disord 2025;26:626. doi: 10.1186/s12891-025-08874-8.
33. Jang SA, Byun YS, Han IH, Shin D. Medial plating of distal femoral fracture with locking compression plate-proximal lateral tibia: Cases' report. J Korean Fract Soc 2016;29:206. doi: 10.12671/jkfs.2016.29.3.206.
34. Kamarudin KI. Medial distal femur fixation with proximal tibial locking plate: A case series. Int e-J Sci Med Educ 2017;11:32-4. doi: 10.56026/imu.11.3.32
35. Zeng ZM, Luo CF, Putnis S, Zeng BF. Biomechanical analysis of posteromedial tibial plateau split fracture fixation. Knee 2011;18:51-4. doi: 10.1016/j.knee.2010.01.006.
36. Silva M, Shepherd EF, Jackson WO, Dorey FJ, Schmalzried TP. Average patient walking activity approaches 2 million cycles per year: Pedometers under-record walking activity. J Arthroplasty 2002;17:693-7. doi: 10.1054/arth.2002.32699.